Allometry, temperature, and the stability of food webs

TECHNISCHE
UNIVERSITÄT
DARMSTADT

Vom Fachbereich Biologie der Technischen Universität Darmstadt
zur
Erlangung des akademischen Grades
eines Doctor rerum naturalium
genehmigte Dissertation von

Dipl.-Biol. Björn C. Rall
aus Bensheim

Berichterstatter (1. Referent): PD Dr. habil. Ulrich Brose
Mitberichterstatter (2. Referent): Prof. Dr. Stefan Scheu
Tag der Einreichung: 16 .Dezember 2009
Tag der mündlichen Prüfung: 12. Februar 2010
Darmstadt 2010
D 17

“Ja, einsam ist der Wissenschaftler, und seine Braut ist die Erkenntnis. “

from “Rumo und die Wunder im Dunkeln” p. 269 by Walter Moers

für meine Eltern

Table of Contents

1. Summary

Understanding the mechanisms driving stability in natural ecosystems is of crucial importance, especially in the current context of global change. A classic paradigm in ecology was that complex food webs (the "who eats whom" of natural ecosystems) should be unstable. This paradigm, however, was based on simple mathematical models. Throughout the last decades, scientists proposed solutions to the contradictions between the predictions of simple models and the observation of the complexity of nature. However, the fundamental mechanisms driving these stabilizing effects are still rather unexplored. Especially, exploring and predicting the reaction of natural ecosystems to changes of the environment is a pressing issue of our time. Forecasting models predicted global warming up to 8°C until 2100, also nutrient enrichment is caused by anthropogenic land use. This causes changes in species composition and may lead to species extinctions.

A fundamental unit of natural ecosystems is the interaction between species. The most obvious interaction is the feeding interaction between a predator and its prey. This interaction is mainly influenced by the metabolism and the feeding rate of the predator, as well as by the population density of the prey. Combining a mechanistic understanding of these interactions and traditional population models led to ground-breaking insights into the mechanisms stabilizing food-webs. For example, a non-random distribution of feeding interactions in a food web increases its resistance against destabilizing effects. This might be caused by strong constraints introduced by the distributions of body masses across the species in a food web. Additionally, relatively weak interactions are known to have a positive effect on stability, if they occur in a specific way within small food-web motifs (e.g., a weak interaction from a top predator to the basal species and a strong interaction to its main prey, the intermediate predator). Also, models suggested that the stability of natural populations may change, if the feeding capacity and the metabolism (or the death rate) of a predator are not equally influenced by the environmental temperature. However, empirical support for this is still scarce.

In this thesis, I explored the impact of body masses and environmental temperature on feeding interactions (Chapters 3.1., 3.2.& 4.1.). Additionally, I explored the influence of these constraints on population and food-web stability by using mathematical models (Chapters 3.3., 3.4., 4.1. & 4.2.).

The body-mass dependence of metabolism generally followed the 3/4 power laws as predicted by the Metabolic Theory of Ecology (Chapter 3.1.). However, the strength of the feeding rates follows a hump-shaped curve with the body mass ratio of the predator to its prey (Chapters 3.1.& 3.2.). This leads to the phenomenon that a predator would not be able to fulfil its metabolic demands if only insufficient small prey would be available (Chapter 3.2.).

Moreover, with increasing temperature, the metabolism increases more than the ability of the predator to consume food (Chapter 4.1.). These findings have fundamental implications for food web stability. Predators only are able to exist within a given range of body mass ratios to their prey. Approximately 97% of all tri-trophic food chains existing in natural food webs fall within this range (Chapter 3.3.). Additionally, at high body-mass ratios an additional interaction from the top predator to the basal species (omnivory) leads to a higher stability when incorporating the results from chapters 3.1. & 3.2. into the population models. Together with the distribution of the interactions as given in natural food webs (Chapter 3.3.), omnivory motifs are stabilised within the whole range of natural body-mass ratios (Chapter 3.4.).

The different temperature dependencies found for metabolism and feeding in chapter 5.1 led to more stable population cycles but may also lead to extinction events caused by starvation of the predators. In addition, warming affects the food web structure, increasing or decreasing these starvation effects, as found in chapter 4.1. Also, enrichment effects on population stability and food-web persistence can be overcome by incorporating naturally plausible feeding interactions (Chapter 5.1.).

Overall, incorporating naturally relevant feeding interactions from laboratory studies into population and food-web models provides important insights into the functioning of populations and their stability in the context of food webs and their response to global change.

2. General Introduction

2.1. Overview

The question of how natural ecosystems can be stable and persistent is one of the oldest and maybe most influential topics in ecology. Especially, in today's context of global change, conservation is more necessary than ever before. To address the problems we are currently facing, a better understanding of how nature functions is fundamental. There are two different ways to address conservation: the first way is to focus on specific species or habitats that seem worth protecting; the second is to adopt general models to understand the impacts of global changes such as nutrient enrichment or global warming.

Natural communities fluctuate in their species compositions and population densities. However, over a longer period of time, ecosystems are persistent. For example, cycles in natural populations of the Canada lynx and the snowshoe hare were already observed in the

Box 3.1.1: Glossary in a nutshell.

Food web: The description of "who eats whom" in a natural ecosystem.

Food-web motif: A small structural unit comprising two to four species.

Functional response: The prey-density dependent per capita feeding rate (see **ingestion rate**) of a one or more predators.

Ingestion rate: Also called feeding rate; the amount of nutriments an animal is consuming within an given amount of time.

Interaction strength: An established expression to describe the strength of an interaction of two species. Usually it describes the feeding interaction. The simplest form is the per capita **ingestion rate**. But also the **functional response** is a measure of interaction strength. A full review on this topic is given in Berlow et al (2004).

Metabolic rate: The amount of nutriments needed by an animal within an given amount of time.

Omnivory: The feeding on more than one trophic levels, e.g. a boar feeds on plants and small invertebrates or acts as an scavenger.

Trophic level: A description of the "height" of a species in a food chain or a food web. A plant would have the trophic level of unity, a herbivore is one step higher than a plant and would have a level of two. A predator feeding on the herbivore would be ranked with an trophic level of three and so on. However, when the predator is omnivorous (e.g. a Grizzly) and feeds on a herbivore and on plants its trophic level would be 2.5. In general, a "prey-averaged" trophic level is calculated by "one plus the average trophic level of the prey".

19th century by the Hudson's Bay Company (Fig. 2.4.1, after Elton & Nicholson 1942). The first simple models describing such population cycles were developed in the 1920s by Alfred J. Lotka (1925) and Vito Volterra (1926). Through time their complexity increased by incorporating more realistic feeding interactions (e.g. a type II functional response (Holling 1959a, b; Real 1977, 1979; Koen-Alonso 2007), see Chapter 2.3. for detailed information) and growth terms (Rosenzweig & Mac Arthur 1963) Later, by taking empirically measured biological rates into account the model was generalised to explore general patterns of natural populations (Yodzis & Innes 1992, but see chapter 2.4. for a detailed introduction to that topic).

In the early 19th century scientists started to describe natural ecosystems by their food-web structure (i.e., the graphical representations of "who eats whom") (Elton 1926). At first, the complexity of food webs was assumed to have a stabilizing effect (MacArthur 1955). Later, Robert May's studies (1972) on complex networks suggested that a higher complexity leads to less stable systems. By adding more and more realistic biological dependencies to their models such as an non-random distribution of the strength of interactions, scientists observed several ways to stabilize complex food-web models (e.g. Yodzis 1981; de Ruiter, Neutel, & Moore 1995; McCann, Hastings, & Huxel 1998). However, today the question remains of why interaction strengths are distributed in a stabilizing way in natural food webs. Using the model provided by Yodzis & Innes (1992) and combining it with food-web models led to the insight that stability increases when the populations within the food web increase in body mass when they are on a higher trophic level (Brose, Williams, & Martinez 2006). This body-mass distribution is also known to be common in nature (Brose et al. 2005a, 2006a). However, the bioenergetic models used in these prior studies are only based on simple metabolic constraints on body mass. But feeding interactions also depend on non-metabolic constraints, i.e. predators cannot feed on prey that is too small prey or prey that is much larger than the predator (Elton 1926, Brose in press). In general predators prefer prey that have an optimal size ratio that maximises the energetic uptake in comparison to the energy they spend searching, catching and handling the prey (MacArthur & Pianka 1966).

Metabolism and feeding interactions do not only depend on body mass but also on the environmental temperature, where increasing temperature leads to higher metabolism, higher moving rates and higher feeding rates (Peters 1983, see Chapters 2.2. & 2.3. for detailed information). In a recent theoretical study, Vasseur & McCann (2005) showed that the differences in temperature dependence between feeding rates and metabolism may affect the stability of a predator-prey system. However, the studies on temperature-dependent feeding rates and their effects on population and food-web stability are scarce.

In my doctoral thesis, I combined techniques from the field of metabolic theory, foraging theory, population biology and food web ecology to investigate the natural patterns that lead to

stable ecosystems. Furthermore, I investigated how external environmental changes, such as warming and nutrient enrichment influence population stability and the survival of species.

More specifically, I measured the metabolic and feeding rates of soil organisms such as beetles and spiders to gain information about how these rates scale with body mass and environmental temperature (Chapters 3.1., 3.2. & 4.1.). These results were used to develop new population and food web models to gain an deeper understanding of how nature can be stable and persistent (Chapters 3.3., 3.4. & 5.1.) and to gain insight into what the effects of anthropogenic induced global change may be (Chapters 4.1. & 4.2.).

2.2. The allometry and temperature dependence of metabolism

One of the most basic biological constraints might be the metabolism of organisms; all movements from molecules up to whole flocks need energy. This energy is gained by burning nutriments. That process was first recognized in the 18th century by the French chemist Antoine Laurent Lavoisier, who is also known as the father of modern chemistry. He was also the first to describe the mechanisms of metabolism (Poirier 1998). About a century later, the first theories were developed about how metabolism scales with animal body mass. Max Rubner (1883) described in experiments using dogs ranging from 3 to 30 kilograms, that the percentage of the nutriment demand decreases with the body mass of the dogs. He explained this phenomenon by the mismatch between the surface and the mass of the body which scales approximately with a power of 2/3. However, this “surface theory” was rejected several times starting with the studies of Max Kleiber (1932, 1947, 1961) who described an increase of metabolism with a 3/4 power law with body mass, called Kleiber's law. Beside the surface theory, other theories where developed to support the often found exponent of 3/4. The “structure theory” takes into account that larger animals have a higher percentage of skeleton to stabilize their body (McMahon 1973). The negligible metabolic activity of the skeleton tissue might explain the allometry of metabolism whereas the bones of a mouse constitute 5% of their body mass and that of elephants 20%. A mathematical description leads to an exponent of 3/4 (McMahon 1973).

The Metabolic Theory of Ecology was based on the fractal organisation of the transport networks of animals and plants (West, Brown, & Enquist 1997, 1999; Brown et al. 2004). The central idea of this approach was to take not only the outer surface into account but also the fractal structure of the inner surfaces like blood vessels in animals or the transport network in plants. This yields an allometric slope of 3/4.

However, allometric exponents range from 0.15 (Zotin & Konoplev 1978) to 1.02 (Kayser & Heusner 1964, summarised in Peters 1983). This led other scientists to propose that every phylogenetic group has adapted its metabolism by evolution. This would not lead to a general valid slope of 2/3 or 3/4 but to a large variance in slopes depending on the evolutionary history of the group of organisms investigated (Kozlowski & Weiner 1997). These different theories were hotly discussed during the last decade (Kozlowski & Konarzewski 2004, 2005; Brown, West, & Enquist 2005; Makarieva, Gorshkov, & Li 2005; Makarieva et al. 2008).

Metabolism also depends on environmental temperature. As metabolism is described by the collectivity of biochemical processes, it should also scale with the average of them (Gillooly et al. 2001). This average slope of the exponential function should have an activation energy of 0.6 to 0.7 (see Box 3.2.1), this was also supported by the data presented in their study. However, other studies showed that the activation energy can vary from 0.2 up to 1.4 (Clarke 2004, 2006; Clarke & Fraser 2004).

Box 3.2.1: *The mathematical description of body mass and temperature dependence of metabolism.*

The allometric and temperature dependency of metabolism, *I*, is usually described by a power law function,

$$I = i_0 M^a e^{\frac{-E}{kT}}$$

where i_0 is a constant, M is the mass of b individual organism, a is the allometric exponent, E is the activation energy, k [eV] is the Boltzmann constant and T is the absolute temperature [K]. A common formulation of that relationship is the linearised form that can be derived by taking the natural logarithm of the basic equation what yields:

$$\ln(I) = a\,M + \ln(i_0) - E(kT)$$

This formulation has two advantages to the first: (1) the scaling allows to show data over many orders of magnitude and (2) the statistical description of a linear model is much easier than that of a non-linear model.

Beside the question of which mathematical model is relevant and what is the right slope of the allometric and temperature relationships, many scientists explored mass-dependent power laws and temperature-dependent exponential functions in all kind of biological rates; like growth rates (Savage, Gillooly, Brown, et al. 2004), biomass production (Ernest et al. 2003) and ingestion rates (Peters 1983; Carbone et al. 1999; Brown et al. 2004), which are directly related to the metabolism, up to global patterns of species abundances (Allen, Brown, & Gillooly 2002; Meehan 2006a). Even more distant natural constraints, such as moving speed, home range and trophic level are (1) describable and (2) mostly derivable from the metabolic equation (summarised in Peters (1983) and Brown (2004)).

2.3. Foraging Theory

In foraging theory, the central description of feeding events is the functional response (Box 3.1.1; Fig. 2.3.1). The first theoretical and empirical framework was introduced by Holling (1959a, b). He presented a mechanistic model that took the handling time, T_h, and the instantaneous search rate, a, into account. The handling time includes the time a predator, i, needs to subdue, ingest and digest its prey, j, as well as resting or cleaning itself (Hassell 1978). The attack rate is an average per capita moving or foraging speed expressed as area or volume successfully searched per time and predator (eg. m² individuals^{-1} day $^{-1}$). With these parameters, the basic mechanistic equation becomes

$$F_{ij} = \frac{a_{ij} N_j}{1 + a_{ij} T_{h_{ij}} N_j} \qquad (2.3.1),$$

which has a hyperbolic shape with increasing prey density (Fig. 2.3.1c) yielding a decreasing predation risk for a single prey item to be hunted with increasing prey density (Fig. 2.3.1d). This basic equation is called type II functional response (Fig. 2.3.1c) and most other more or less complex functions can be derived from it (Jeschke, Kopp, & Tollrian 2002). Beside the type II functional response, the other basic curves are the type I functional response (Fig. 2.3.1a) which shows a linear increase of the feeding rate, yielding a constant predation risk for the prey (Fig. 2.3.1b); the type III functional response (Fig. 2.3.1e) that has a sigmoid shape with prey density, yielding a hump-shaped predation risk for a single prey item (Fig. 2.3.1f); and the predator-interference functional response, which takes the density and interaction of the predators into account (Fig. 2.3.1g), and where the predation risk for a single prey decreases

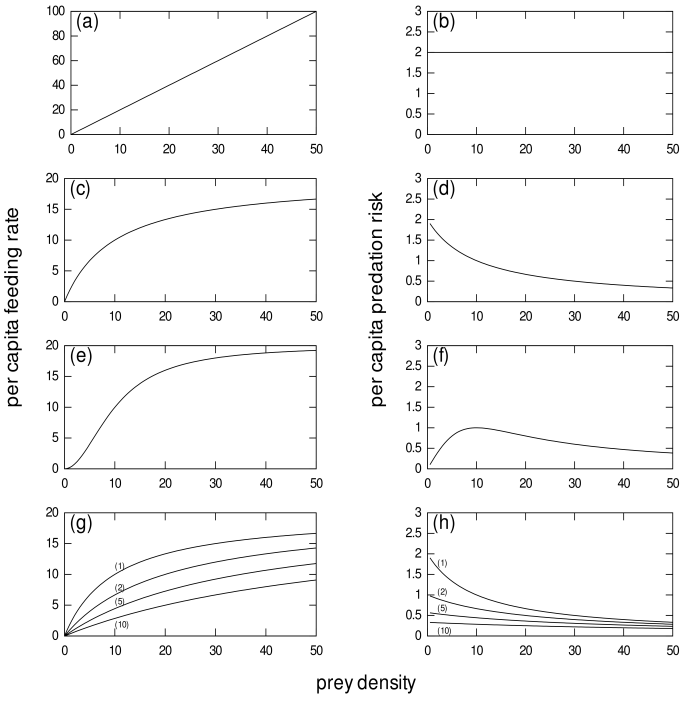

Figure 2.3.1: The shapes of the functional response models type I **(a)**, type II **(c)**, type III **(e)** and the predator interference functional response **(g)**. The right column displays the according per capita predation risks (feeding rates divided by prey density) for one prey individual **(b, d, f, h)**.

with increasing predator density (Fig. 2.3.1h).

The type I functional response is maybe the oldest description of a prey-dependent feeding interaction that follows a simple linear increase with prey density (Fig. 2.3.1a). The mechanistic explanation for a type I functional response is the simplifying assumption that the handling time (Eqn. 2.3.1) approaches zero.

$$F_{ij} = a_{ij} N_j \tag{2.3.2}$$

This assumption can be made if the predator is able to forage while he is consuming and digesting. Animals that are much larger than their prey, such as filter feeders, are that kind of predators and assuming that the filtering rate follows the environmental density of prey items, the functional response becomes linear (Jeschke, Kopp, & Tollrian 2004). A more recent study suggested that a type I functional response is wrong, because most studies ignore relatively low densities or extremely high densities of prey (Sarnelle & Wilson 2008). They showed that if these gaps of density are filled, the feeding curve becomes sigmoidally shaped, which implies a type III functional response.

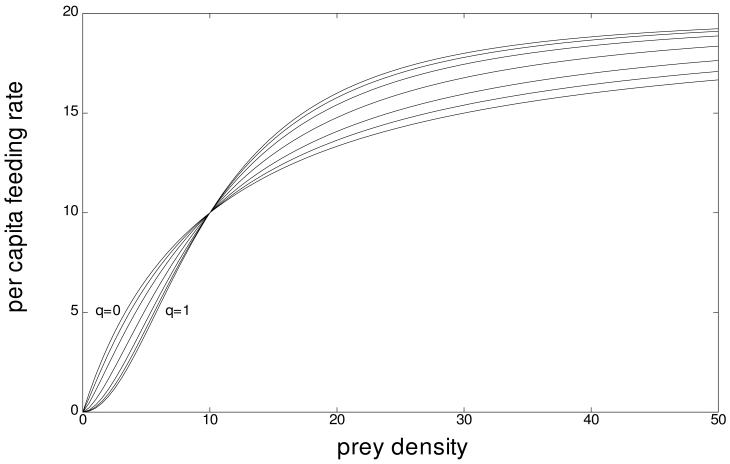

Figure 2.3.2: Different shapes of the functional response varying from $q = 0$ to $q = 1$.

The type III functional response assumes that the attack rate is not a constant but prey-density dependent. The simplest form of that is a linear increase of the attack rate:

$$a_{ij} = b_{ij} N_j \tag{2.3.3},$$

where b_{ij} is the attack coefficient and N_j is the prey density. This yields the following functional response:

$$F_{ij} = \frac{b_{ij} N_j^2}{1 + b_{ij} T_{h_{ij}} N_j^2} \tag{2.3.4}$$

which has a sigmoid shape (Fig. 2.3.1e). The linear increase of the attack rate may not be enough to describe the complexity of the functional response. The attack rate can become an even more complex function of prey density (Juliano 2001). However, most of that attack-rate

models lack in statistical applicability. Real (1977, 1979) presented an elegant way to describe the prey-density of the attack rates by introducing the Hill exponent, *h*, to the functional response model. The Hill exponent was adopted from enzyme kinetics (Barcroft & Hill 1910)

$$F_{ij} = \frac{b_{ij} N_j^h}{1 + b_{ij} T_{h_{ij}} N_j^h} \qquad (2.3.5)$$

In this functional response model, the attack rate becomes

$$a_{ij} = b_{ij} N_j^q \qquad (2.3.6)$$

where the *q*-exponent equals the Hill exponent minus one ($q=h-1$) (Williams & Martinez 2004a). This description of the functional response is more flexible than distinct attack-rate models (Juliano 2001) and allows a continuous shape of the functional response from a strict type II to a type III functional response (Fig. 2.3.2).

The question of how feeding is related to the prey density is not the only one in foraging theory. The predator density is also important to understand the feeding relationships (Skalski & Gilliam 2001). Increasing predator density leads to more competition among predators as well as miscellaneous other activities such as mating or eventually social interactions. These interferences can be included in the functional response in several ways, whereas the easiest was tested to be the best (Skalski & Gilliam 2001). In this so called Beddington-De Angelis functional response, a simple interference term ω_i is added to the model yielding (Beddington 1975; De Angelis, Goldstein, & O'Neill 1975):

$$F_{ij} = \frac{a_{ij} N_j}{1 + \omega_i N_i + a_{ij} T_{h_{ij}} N_j} \qquad (2.3.7a).$$

Using this interference term in the generalized type III functional response leads to:

$$F_{ij} = \frac{b_{ij} N_j^h}{1 + \omega_i N_i + b_{ij} T_{h_{ij}} N_j^h} \qquad (2.3.7b).$$

In addition to the time spent handling and searching, a predator spends time interacting with other intra-specific individuals which yields a decreased per capita feeding rate with increasing predator density (Fig. 2.3.1g). There are many other formulations of interference existing in the literature, but see Chapter 5.1. b) and the paper by Abrams & Ginzburg (2000) for a detailed discussion on that topic.

Beside these mechanistic approaches, Real (1977, 1979) introduced an often used phenomenological version of the functional response. It comprises maximum ingestion rates J_{max} and half-saturation densities N_0 instead of handling times and attack rates:

$$F_{ij} = \frac{J_{max} N_j^h}{N_0^h + N_j^h} \quad (2.3.8a);$$

$$F_{ij} = \frac{J_{max} N_j^h}{N_0^h + \omega_i N_i + N_j^h} \quad (2.3.8b).$$

This is especially convenient if functional responses are calculated from field observations, as often done in marine sciences (e.g. Smout & Lindstrom 2007). Also, many theoretical studies use similar functional responses to predict macro-ecological patterns such as population dynamics and food web persistence (e.g. Yodzis & Innes 1992; McCann & Yodzis 1994; McCann & Hastings 1997; McCann et al. 1998; Williams & Martinez 2004a; Brose, Berlow, & Martinez 2005; Brose et al. 2006b; Rall, Guill, & Brose 2008).

With the following assumptions, the mechanistic models (Eqn. 2.3.7) can be derived from the phenomenological one and *vice versa*:

$$J_{max} = \frac{1}{T_h} \quad (2.3.9a);$$

$$N_0 = \frac{1}{a T_h} \quad (2.3.9b).$$

For a detailed description of these derivations, see Chapter 3.4. b).

All functional response models presented so far only describe one predator – one prey interactions. In natural food webs, however, prey have several predators and predators have many prey species. A generalized description of a multi-species functional-response model was provided by Murdoch & Oaten (1975). The model considers the time a predator spends foraging on other prey as follows:

$$F_{ij} = \frac{b_{ij} N_j^h}{1 + b_{ij} T_{h_{ij}} N_j^h + \sum_{k=1}^{k=n} b_{ik} T_{h_{ik}} N_k^h} \quad (2.3.10).$$

The phenomenological version of the model can also be written in a multi-species version (Koen-Alonso 2007):

$$F_{ij} = \frac{\Omega_{ij} J_{max} N_j^h}{N_{tot} + \Omega_{ij} N_j^h + \sum_{k=1}^{k=n} \Omega_{ik} N_k^h} \quad (2.3.11),$$

where N_{tot} is the total half-saturation density and Ω_{ij} is the weight factor of the predator to a specific prey. The weight factor can be derived by dividing the prey specific attack rate by the

sum of all attack rates. The total half-saturation density is calculated by the maximum ingestion rate divided by the sum of all specific attack rates (see Koen-Alonso 2007 and Chapter 3.4. b) for details).

2.4. Theoretical Ecology – from populations to food webs

Population Biology has a long standing history starting with early observations of the abundances of the Canadian lynx in the 19th century (Fig. 2.4.1). The Hudson's Bay Company counted the returning furs of the lynx by their trappers, and Elton & Nicholson (1942) investigated the data to create a time series that is longer than 100 years. This early dataset is still explored and extended by scientist (e.g. Bulmer 1974; Krebs et al. 2001; Roth et al. 2007; Vik et al. 2008). These ten-year population cycles of the lynx were interpreted as the numerical reaction to the abundance of its main prey, the snowshoe hare. To explain such cycles, scientists developed mathematical models already in the 1920's (Lotka 1925; Volterra 1926). The Lotka-Volterra model made simple assumptions like an exponential growth of the prey species and a linear type I functional response. Later, Rosenzweig & MacArthur (1963) replaced these simple assumptions with a logistic growth (a species can grow to a maximum according to a hump shaped curve) and a saturating type II functional response (see Chapter 2.3.). These substantial components of the Rosenzweig-MacArthur model are still used in recent studies to explore population dynamics. One further step was to include general mechanisms and scalings to the population models. Based on the Rosenzweig-MacArthur model, Yodzis & Innes (1992) developed a body-mass dependent population model that was based on macro-ecological rates of production, feeding and metabolism. Additionally, by expressing every rate relatively to the growth rate and all spatial rates relatively to the carrying capacity of the basal species they generalized the model (but see Chapters 3.4. and 5.1. for a detailed description). With Yodzis & Innes model, many studies on small food web motifs (e.g. the three species food chain, omnivory and competition motifs) were carried out (e.g. McCann & Yodzis 1994; McCann & Hastings 1997; McCann et al. 1998) which influenced and stimulated ecological research.

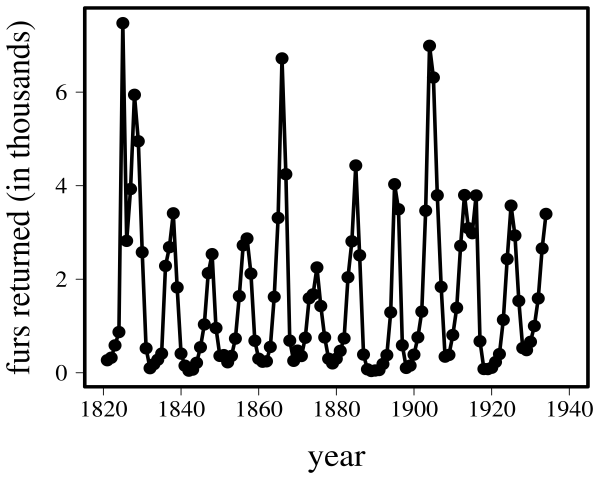

Figure 2.4.1: The population cycle of the Canadian lynx as reported by Elton & Nicholson (1942). The x-axis represents the years from 1820 to 1940 and the y-axis denotes the lynx furs returned to the Hudson's Bay Company from the area of the MacKenzie River District. (Data from Elton & Nicholson (1942); Table 4)

Generally, the methods to explore the dynamical output of population models are numerous. The simplest method is the graphical inspection (Fig. 2.4.2) provided by Rosenzweig and MacArthur (1963).

First, a population model has to be created. In a two species system, two equations are drawn; one for the resource species (referred to as the basal or prey species) and one for the consumer species (or predator species). These equations comprise (1) a growth term for the basal species that includes growth and intraspecific competition; (2) a feeding interaction between the species, expressed as the functional response of the consumer on the resource species; and (3) a loss term of the predator species according to death or metabolism of the consumer:

$$\frac{dN_i}{dt} = N_i G_i - N_j F_{ij} \qquad (2.4.1a)$$

$$\frac{dN_j}{dt} = N_j F_{ij} - z_j N_j \qquad (2.4.1b),$$

where G_i is the growth rate of the resource species and z_j is the death rate of the consumer. For example, using a type II functional response for the feeding rate F_{ij} and a logistic growth for the growth term G_i yields

$$\frac{dN_i}{dt} = N_i r_i \left(1 - \frac{N_i}{K}\right) - \frac{a_{ij} N_i}{1 + a_{ij} T_{h_{ij}} N_i} N_j \qquad (2.4.2a)$$

$$\frac{dN_j}{dt} = \frac{a_{ij} N_i}{1 + a_{ij} T_{h_{ij}} N_i} N_j - z_j N_j \qquad (2.4.2b)$$

In a second step, the assumption is made that both populations exhibit equilibrium dynamics (the population densities do not change through time; $dN_i/dt = dN_j/dt = 0$). The equations can be rewritten and simplified to get the resource and consumer isoclines:

$$N_j = -\frac{a_{ij} r_i T_{h_{ij}} N_i^2 + (r_{ij} - a_{ij} r_i T_{h_{ij}} K_i) N_i - r_i K_i}{a_{ij} K_i} \quad (2.4.3a),$$

$$N_i = \frac{-z_j}{a_{ij} z_j T_{h_{ij}} - a_{ij}} \quad (2.4.3b).$$

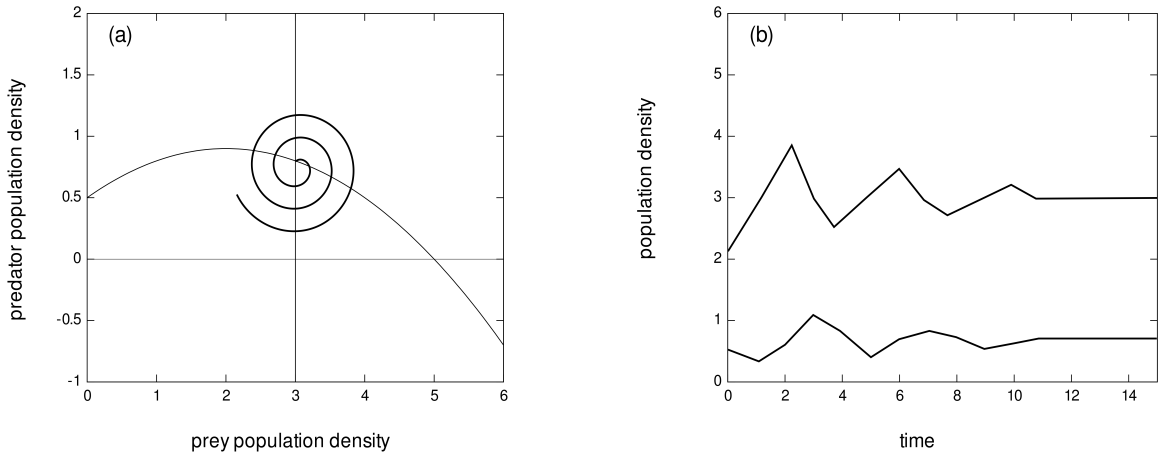

Figure 2.4.2: Graphical representation of the equations (2.4.3a,b). Plot **(a)** displays the phase space of the prey population (x-axis) and the predator population (y-axis). The spiral displays the time-dependent population densities of both populations. **(b)** Mirroring the values of that spiral into a plot, where the time is the x-axis and the population density is the y-axis yields the time series of both species, whereas the predator yields a lower population density than the prey.

In these equations, the population densities of the predator species follow a quadratic function depending on the prey density and the prey density follows a straight line depending on the death rates of the predator and on the functional response parameters. The graphical solution is presented in the so-called phase-space diagram (Fig. 2.4.2a). Imagine a starting population size of approximately 2.2 for the resource species and of approximately 0.4 for the predator density. The population dynamics follow a circular behaviour counter-clockwise (spiral in Fig. 2.4.2a). The parameters are chosen so that the time series follows a spiral trajectory towards the intersection of both isoclines. From this analysis, the population cycles through time can be drawn into a second graph (Fig. 2.4.2b). However, there are several problems using this approach. Exploring large gradients of parameters would cause an infinite set of phase-space diagrams. For this reason, many studies also use a graph plotting two parameters of interest (e.g. body mass and temperature) while indicating the parameter space in which (1) the system is feasible, and (2) the system will exhibit non-equilibrium dynamics. The boundaries between the different areas are called feasibility boundary and Hopf boundary (Yodzis & Innes 1992), but see Chapter 5.1. d) for a detailed derivation of these boundaries.

Box 3.4.1: *From time series to bifurcation diagrams*

The dynamical behaviour of single populations is the most simple example for displaying principles of population biology. May (1974) investigated the behaviour of a single population with a distinct population model following the equation:

$$N_{(t+1)} = \lambda N_{(t)}[1 - N_{(t)}]$$

where N(t) is the population density at the time t and λ is the intrinsic growth term. By increasing the growth term, λ, the population begins to fluctuate (Fig. 2.4.3, small displays) where at a value of λ = 2, the population yields an equilibrium dynamic, at a value or λ = 3.3 a limit cycle dynamic what means that the population fluctuates between two definite values. At λ = 3.5, the limit cycles show two maxima and two minima, whereas at λ = 4 the population is in a non-predictable chaotic state. To investigate a continuum of λ-values, using a bifurcation diagram is a common method (Fig. 2.4.3, large display). Until a value of approx. λ = 3.0, the population dynamics are in an equilibrium state, crossing the first bifurcation point (from the Latin name furca = fork), the population dynamics increase in amplitude, until more and more bifurcation points are reached and the dynamics become chaotic.

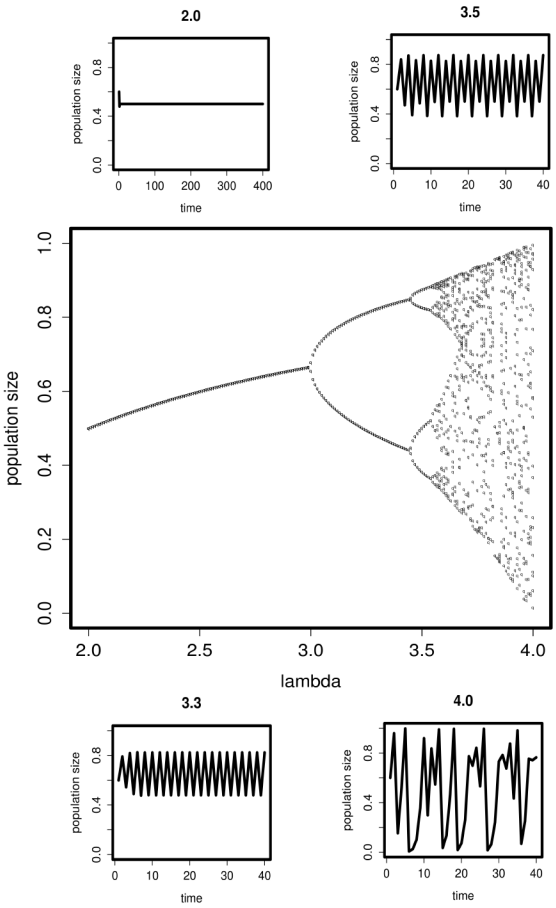

Figure 2.4.3: The small plots show selected time series of a single population (Box 3.4.1). The main plot displaying the minima and maxima of those time series, describing the "route to chaos" (from: Crawley 2007) with increasing intrinsic growth of the species.

A major problem arises from these kinds of analyses. The simplifying assumption that populations are at an equilibrium state is often false, especially when the model contains more than two species, but even with less species the populations often exhibit non-equilibrium dynamics (May 1974, see Fig. 2.4.3 for an example). With increasing computational power scientists targeted to solve population equations (e.g. Eqn. 2.4.2a,b) numerically. To investigate the dependency of the population densities and stability on one or more parameters, many time series have to be simulated and only the minima and maxima of the population densities are saved. The minima and maxima will be transferred into so called bifurcation diagrams yielding a scatter plot (see Box 3.4.1 for a worked example). This common method gave interesting insights into how interaction strength of feeding interactions influences the stability of the populations. For example, tri-trophic food chains where thought to exhibit equilibrium dynamics because the parameters leading to chaotic dynamics where biologically unlikely (Hassell, Lawton, & May 1976) and where thought to be introduced by

human impact (Berryman & Millstein 1989). Later studies showed that there is evidence for chaotic dynamics in tri-trophic food chains in theoretical studies within biological relevant parameters (Hastings & Powell 1991; McCann & Yodzis 1994a), empirical experiments (Beninca et al. 2008), and might not only due to human impact such as enrichment (McCann & Yodzis 1994b). From this turning point of population modelling, the question came up, why natural populations are able to co-exist in a relatively non-chaotic way. By adding an additional feeding interaction from the top predator of this tri-trophic food chain to the basal species (creating an omnivorous top predator), McCann & Hastings (1997) showed that with a specific set of parameters, the chaotic dynamics found in the food chain were reduced to equilibrium dynamics. With this study, they solved two problems in one step: omnivorous motifs tended to become simple predator-prey systems, as the top predator out-competes the intermediate or *vice versa*. However, more general studies showed that the space of possible biological relevant parameters also allows scenarios where chaotic dynamics or out-competing occur more often than the system is stabilized (Holt & Polis 1997; Vandermeer 2006). Despite the lack of empirical evidence and generality of the existence of weak interactions, the concept that weak interactions have the power to stabilise populations was extended and generalised to more complex structural motifs and to whole food webs (McCann et al. 1998; Neutel, Heesterbeek, & de Ruiter 2002).

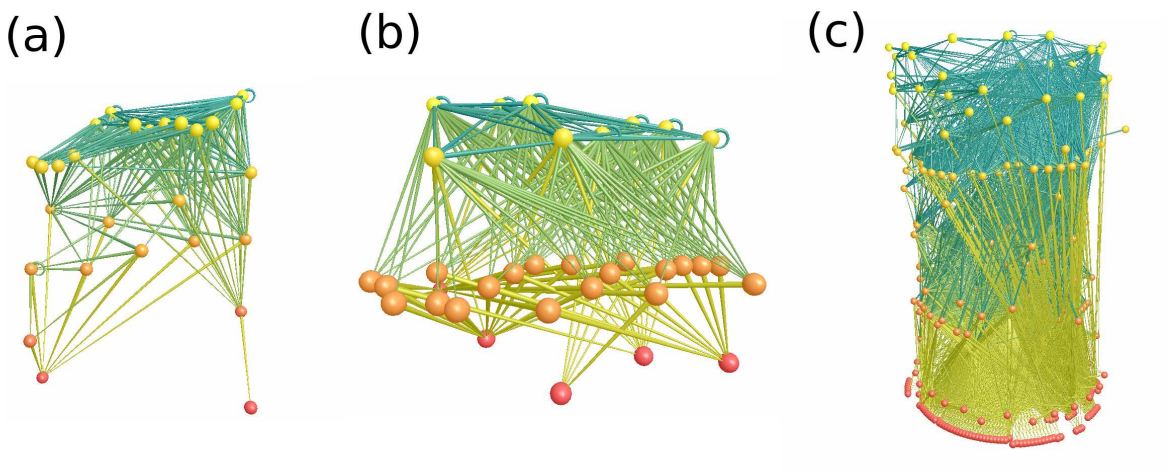

Figure 2.4.4: Visualizations of empirical measured food webs; **(a)** the Benguela Marine System (Yodzis 1998) as an example for an food web that has a low number of species and a low number of feeding interactions; **(b)** the Broadstone Stream food web (Woodward, Speirs & Hildrew 2005), a highly connected food web with a small number of species, in Chapter 3.4.; **(c)** the Weddell Sea marine food web (Brose et al. 2005a), the to date largest measured food web with over 500 species. Image produced with FoodWeb3D, written by R.J. Williams and provided by the Pacific Ecoinformatics and Computational Ecology Lab (www.foodwebs.org, Yoon et al. 2004).

The investigation of food-web stability is challenging. Food webs comprise several populations that feed on each other (e.g. Fig. 2.4.4). Because of the high number of species and their interactions, the graphical and analytical analyses presented in the previous paragraphs are not usable. This led to many simplifications in the analyses, e.g. a linear interaction term (attack rate, see above). Despite all these simplifications, early stability investigations of food webs showed that increasing complexity (the number of species or the number of feeding interactions) leads to a decreased probability of stability in the food web (Gardner & Ashby 1970; May 1972). However, the structure of the investigated webs was extremely artificial, as a random structure was assumed. With increasing interest on food-web structure within ecological sciences, ecologists measured the food web structure of real food webs [e.g. the marine food-web from Benguela (Yodzis 1998); the freshwater food web Broadstone Stream, U.K. (Woodward, Speirs, & Hildrew 2005); and the today's largest measured food-web, Weddell Sea (Brose et al. 2005a); Fig. 2.4.4, image produced with FoodWeb3D, written by R.J. Williams and provided by the Pacific Ecoinformatics and Computational Ecology Lab (www.foodwebs.org, (Yoon et al. 2004)]. Analyses of these food webs showed that the structure is not random but follows strong constraints (e.g. Martinez 1991). Also the distribution of the strength of the interactions is non-random. Stability analyses of such food webs also showed an increased resistance against perturbations than random networks (e.g. Yodzis 1981; de Ruiter, Neutel, & Moore 1995, 1998). With the increasing knowledge of food-web structure, the question arised how structure can emerge from general natural patterns. This led to the development of several structural food web models that first followed simple stochastic principles (Cohen, Briand, & Newman 1990; Williams & Martinez 2000), but became more and more mechanistic by trying to include e.g. phylogenetic traits (Cattin et al. 2004). Using these and similar models and combining them with numerical population models led to deep insights into how stability is influenced by the shape of the functional response or allometric constraints given by the Metabolic Theory of Ecology (Williams & Martinez 2004a; Brose et al. 2006b).

2.5. Contributions to the included articles

Chapter 3.1.: Foraging theory predicts predator–prey energy fluxes

Authors: Brose, U., Ehnes, R., Rall, B.C., Vucic-Pestic, O., Berlow, E. & Scheu, S.

Published in: Journal of Animal Ecology (2008), Vol. 77, pp. 1072-1078; doi: 10.1111/j.1365-2656.2008.01408.x

U.B., R.E., B.C.R and O.V.P. had the Idea and carried out the experiments. Statistical analyses by U.B. and B.C.R., the text was written mainly by U.B., E.B. and S.S. with minor

contributions of R.B., B.C.R. and O.V.P..

Chapter 3.2.: Allometric functional response model: body masses constrain interaction strengths

Authors: Vucic-Pestic, O., Rall, B.C., Kalinkat, G. & Brose, U.

Published in: Journal of Animal Ecology (2010), Vol. 79, pp. 249–256; doi: 10.1111/j.1365-2656.2009.01622.x

Idea by O.V.P, B.C.R. and U.B., laboratory work by all authors; statistical analyses by O.V.P & B.C.R.; the text was written mainly by O.V.P., B.C.R. and U.B. with minor contributions of G.K..

Chapter 3.3.: Allometric degree distributions facilitate food web stability

Authors: Otto, S., Rall, B.C. & Brose, U.

Published in: Nature (2007), Vol. 450, pp. 1226-1229; doi: 10.1038/nature06359

All authors contributed equally to this paper.

Chapter 3.4.: The omnivory conundrum: allometry balances weak and strong interactions in complex food webs

Rall, B.C., Binzer, A., Kefi, S., Schneider, F.D., Woodward, G. & Brose, U.

in preparation

Idea by B.C.R. and U.B.; establishing the theoretical model by B.C.R., U.B., A.B., F.D.S., empirical data by G.W., statistical analyses by B.C.R.; text by B.C.R., S.K. & U.B. with minor contributions of the other authors.

Chapter 4.1.: Temperature, predator-prey interaction strength and population stability

Rall, B.C., Vucic-Pestic, O., Ehnes, R.B., Emmerson, M.C. & Brose, U.

Published in: Global Change Biology, in press.; doi: 10.1111/j.1365-2486.2009.02124.x

Idea by B.C.R., laboratory work by B.C.R., O.V.P., R.B.E. & U.B.; statistical analyses and theoretical analysis by B.C.R.; the text was written mainly by B.C.R., M.C.E. and U.B..

Chapter 4.2.: Predicting the effects of temperature on food web connectance

Petchey, O.L., Brose, U. & Rall, B.C.

submitted

Idea by all authors, statistics and model evaluation by O.L.P. & B.C.R; Text mainly by O.L.P. with minor contributions of U.B. & B.C.R.

Chapter 5.1.: Food-web connectance and predator interference dampen the paradox of enrichment

Rall, B.C., Guill, C. & Brose, U.

Published in Oikos (2008), Vol. 117, pp. 202-213; doi: 10.1111/j.2007.0030-1299.15491.x

Idea by B.C.R. & U.B.; numerical analyses by B.C.R., analytical analyses by B.C.R. & C.G. (analytical solutions for the Hopf boundaries by C.G.); text by all authors.